SMiRT-12 / K. Kussmaul (Editor)
1993 Elsevier Science Publishers B.V.

L04/1

A DISLOCATION MODEL OF PLASTIC YIELD IN FUEL PIN CLADDING MATERIALS

I.J. Ford

Theoretical Studies Department, AEA Industrial Technology, B424.4, Harwell Laboratory, Didcot, Oxon, OX11 0RA, UK

ABSTRACT

A mechanistic understanding of plastic yield is developed using ideas of dislocation dynamics, and is applied to the interpretation of tensile test data for candidate fast reactor fuel pin cladding materials. The central ingredients of the model are rate equations describing the evolution of the mobile and static components of the dislocation density, and a physical model of the mobilisation mechanism. The model can account for the temperature, strain and strain rate dependence of the yield stress, using values for the physical parameters obtained by fitting predictions to experiment, and extension to irradiation effects and recovery/recrystallisation is straightforward. The model also offers the prospect of development to include creep plasticity.

1. INTRODUCTION.

The modelling of fuel pin behaviour requires an adequate description of plastic yield in order to describe deformation which may occur in hypothetical accident conditions. Depending on the circumstances, plastic yield could accommodate and relax any applied stresses, or alternatively, lead to the failure of the pin. The main material parameter which describes yield is the yield stress σ_y. Failure analyses have traditionally used empirically based fits for σ_y as a function of the key parameters of temperature, strain and strain rate, but it is necessary to go beyond this treatment if transient situations are considered where these parameters are changing. The best way of providing this is to develop a physically based model of plasticity, containing a realistic description of the phenomena responsible for deformation.

Plasticity is a consequence of the motion of dislocations within the material. The generation and evolution of the dislocation population is a complicated matter, however, and a model taking into account all possible processes would be unnecessarily detailed. The approach taken here is to use the simplest dislocation models consistent with the general features of experimental data for the yield behaviour materials of interest. The tensile test data used [1] is described in Section 2, and a simple interpretation offered in Section 3 for both the yield stress and the hardening behaviour. A numerical model based on rate equations for the evolution of static and mobile dislocation populations is proposed and developed [2,3]. Conclusions are given in Section 4.

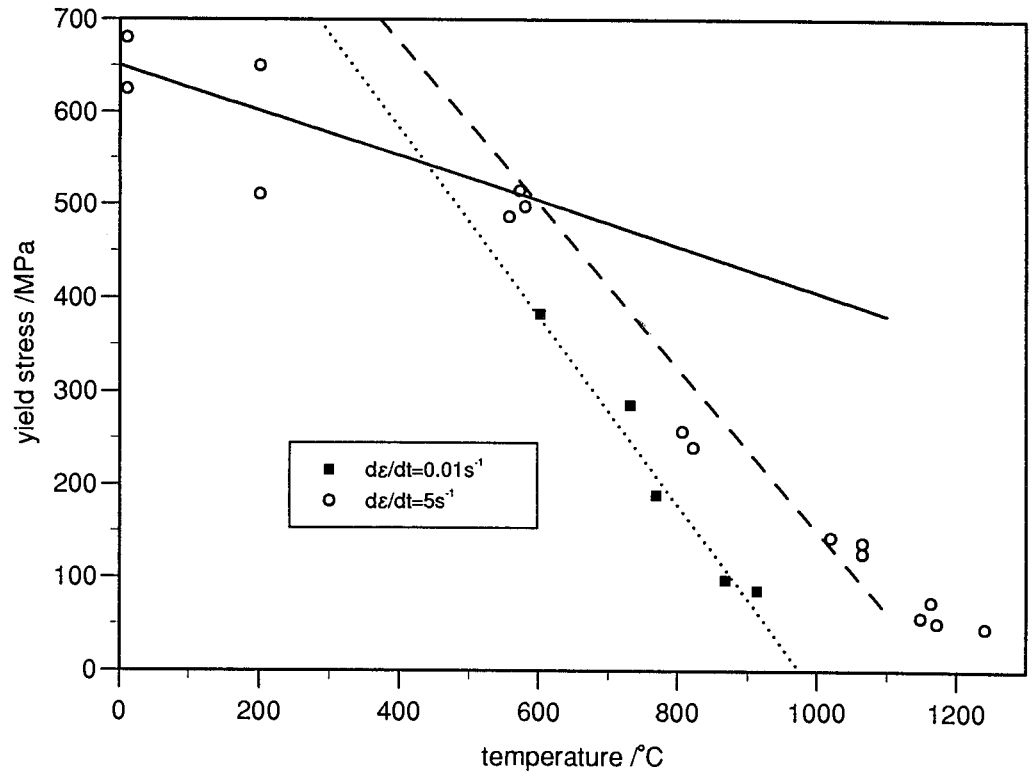

Figure 1. Yield stress data for 20% cw AISI 316 steel, at temperatures reached at very rapid heating rates (>200K/s) [1]. Lines are calculated fits.

2. TENSILE DATA.

We concentrate on the yield behaviour of 20% cw AISI 316 austenitic stainless steels which has been used as the cladding material for fast reactor fuel pins, and for which an extensive database of materials properties exists. The tensile properties of this material have recently been studied within the CABRI-1 project [1], providing a valuable source of data for model building. The design of the tests, involving fast heating rates to the test temperature and rapid strain rates during the test, has clarified the role of each parameter in determining the yield stress. Slow tests at high temperatures run the risk of introducing thermal recovery effects which might confuse the interpretation.

The temperature and strain rate dependence of the yield stress of the unirradiated material is shown in Figure 1. The data shown were obtained at high rates of heating to the test temperature, minimising the effects of recovery [1]. Two linear sections provide a good fit to the yield stress at each strain rate. The data show a strong temperature and strain rate dependence at high temperature, but only a weak dependence on temperature at low temperature. The measured yield stresses can be described by the following expression:

$$\sigma_y = \min(\ A\mu - BT\ln(C/\dot{\epsilon})\ \ ,\ \ D\mu\ )\ \ , \tag{1}$$

where μ is the shear modulus, given by:

$$\mu = 8.54 \times 10^4(1 - 3.143 \times 10^{-4}T) \text{ MPa} \quad (2)$$

T is the absolute temperature and A, B, C and D are constants (0.0148, 0.0221, 2.62×10^9 and 0.0084, respectively, with σ_y in MPa, T in K and $\dot{\epsilon}$ in s^{-1}).

The strain-hardening of the cladding material is also important in determining the accommodation of strains. The experiments have provided a limited amount of data describing the dependence of the yield stress on strain, and this is described in the next section.

3. DISLOCATION DYNAMICS.

The plastic deformation of a material results from the flow of dislocations within it. This can be achieved either by increasing the stress so that the forces resisting motion are exceeded (athermal mobilisation), or by increasing the temperature sufficiently so that the energy barriers against flow can be overcome by thermal fluctuation, or avoided by non-conservative dislocation motion brought about by the mobilisation and absorption of vacancies (thermal mobilisation). Once brought into motion, dislocations can interact, leading to annihilation if the mutual orientations are suitable, or to tangling, whereupon further motion ceases. A number of models of dislocation dynamics have been proposed [4-12], often based on rate equations describing the evolution of various populations. In this paper, a new model of the dynamics is developed, which is then used to interpret a number of experimental features.

Plastic deformation is often divided into time dependent and time independent components, referred to as creep and yield (or sometimes simply plasticity) respectively. These components can be associated loosely with the athermal and thermal mobilisation mechanisms, respectively, referred to above. However, at high temperatures especially, the distinction between the two becomes blurred, as manifested by an emerging strain rate sensitivity of the yield stress, and it is better to treat all mechanisms together in a unified model. The model described below is a development along these lines.

3.1 Dislocation mobilisation.

Consider a dislocation pinned at various points along its length, as illustrated in Figure 2. The pinning prevents the dislocation gliding and producing strain. As the stress increases, however, the dislocation bows out between the pinning points, as shown. The yield stress corresponds to the stress at which the dislocation escapes from restraint, and depends on the restraining force at the pinning point. Let the dislocation line tension be τ, and the maximum restraining stress exerted on the dislocation at the pinning points be $\alpha\tau$. Under a stress σ, the dislocation bows out between pinning points until the cusp angle ϕ between adjacent bowed segments is given by

$$\sigma = 2\tau \cos\phi/2 = \frac{\mu b}{\ell} \cos\phi/2 \quad , \quad (3)$$

where b is the Burgers vector and ℓ is the distance between pinning points (assumed constant). If $\alpha < 2$, then at some σ, the pinning force is overcome and the restraint on

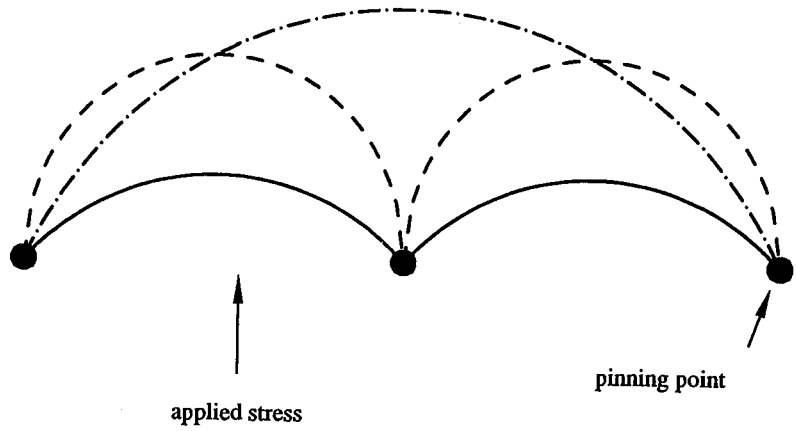

Figure 2. Initial dislocation (solid line), bowed dislocation (dashed line)

the dislocation is broken. Let us, however, consider the case where $\alpha > 2$ so that the pinning point is impenetrable under stress alone. In these circumstances, escape is only possible by the Orowan mechanism, whereby the dislocation surrounds the pinning point and breaks away leaving a loop. In the absence of thermal fluctuations, this corresponds to a yield stress σ_y equal to $\mu b/\ell$, which is weakly temperature dependent, through μ, and strain rate independent.

However, thermal fluctuations alter the situation and allow penetration of the pinning points. At a given applied stress σ and an equilibrium configuration characterised by a cusp angle $\phi > 0$, the free energy barrier against the penetration of the obstacle, according to a simple model [6] where the resistive force is constant over a distance d, is:

$$\Delta G = \frac{\alpha \mu b^2 d}{2}\left(1 - \frac{2}{\alpha}\cos\phi/2\right) \quad , \tag{4}$$

and the strain rate which arises from cutting the obstacle is then

$$\dot{\epsilon} = \rho b \ell \nu \exp\left(-\Delta G/kT\right) \quad , \tag{5}$$

where ν is the attempt frequency and ρ is the density of dislocations held up at such pinning points. The stress required to produce a given strain rate $\dot{\epsilon}$ is therefore

$$\sigma = \frac{\mu b \alpha}{2\ell} - \frac{kT}{\ell b d}\ln\left(\frac{\rho b \ell \nu}{\dot{\epsilon}}\right) \quad . \tag{6}$$

In this simple model, therefore, the yield stress is given by

$$\sigma_y = \frac{\mu b}{\ell}\min\left\{ \frac{\alpha}{2} - \frac{kT}{\mu b^2 d}\ln\left(\frac{\rho b \ell \nu}{\dot{\epsilon}}\right) \quad , \quad 1 \right\} \quad , \tag{7}$$

which has clear similarities with the experimental fit eq.(1). Considering the simplicity of the model, this is a little surprising; but we shall take the model as the basis of our interpretation. Identifying the empirical constants A-D with the various parameter combinations in eq. (7), and assuming that $\rho = \ell^{-2}$, reasonable values for the physical parameters may be found. Using $b = 0.257$ nm, the procedure yields $\alpha = 3.52$, $\nu = 3.1 \times 10^{11}$ s^{-1}, $\ell = 31$ nm and $d = 0.08$ nm. Note that $\alpha > 2$, as required. In real materials, pinning distances and restraining forces vary, which leads to a smoother change in slope as the temperature increases [4-6], but the simple linear fit is adequate here. Note that the combination of athermal and thermal flow mechanisms represents a step towards the combined treatment of creep and yield plasticity, in line with earlier comments.

The dislocation escapes by whichever mechanism requires the lower stress. At low temperatures, the obstacles are impenetrable and the dislocation escapes by the Orowan mechanism. At higher temperature, however, obstacle penetration is made possible by thermal fluctuation. Hence the low temperature yield stress is strain rate independent and only slightly temperature dependent, whereas the high temperature yield stress depends strongly on both parameters. The change in slope in Figure 1 corresponds to the crossover between the two mechanisms. The crossover point is strain rate dependent.

A similar analysis of thermally excited flow has been used previously to explain an opposite situation which is thought to apply at very low temperatures: a strongly temperature and strain rate dependent yield stress at low temperatures and a less sensitive yield stress at higher temperatures [6]. The important new element in the model here is the competition between obstacle penetration and Orowan bypassing, rather than the simple thermal or athermal penetration of the obstacle, and the important differentiating feature is that $\alpha > 2$.

In the next section we shall apply these ideas in a description of the evolution of various dislocation populations.

3.2 Dislocation immobilisation.

In order to account for the strain dependence of the yield stress (the strain-hardening behaviour), it is necessary to consider the population dynamics of dislocations, taking into account rates of mobilisation, immobilisation, and the changing resistive forces. Homogeneity and isotropy is assumed, so that a single node calculation of populations is sufficient.

The starting point is the Orowan equation:

$$\dot{\epsilon} = b\rho_m v \quad , \tag{8}$$

where ρ_m is the density of mobile dislocations, i.e. those actually in motion, or temporarily held up at an obstacle, and v is their velocity. The remaining dislocations will be described as static, with density ρ_s. Both populations give rise to forces resisting further motion. The following interpretation of the effects of the two populations is offered.

The static dislocations exist as an immovable tangle, and simply present pinning points to restrain the mobile dislocations. The restraining forces are short range, and can be

treated using the model described in the last section. The mobile dislocations, however, even those temporarily held up, retain their long range stress fields, and present a long range stress opposing dislocation motion relative to themselves. The back stress is proportional to $\mu b \rho_m$. The total yield stress is therefore the sum of two components:

$$\sigma_y = \beta_m b \mu \rho_m^{1/2} + \beta_s b \mu \rho_s^{1/2} \mathcal{F} \quad , \tag{9}$$

where $\beta_{m,s}$ are dimensionless constants of the order of unity and $\mathcal{F}$ is the minimum function in eq. (7). The appearance of $\mathcal{F}$ underlines the fact that only the resistance due to the static population can be overcome thermally since only these restraining forces are short range. The empirical success of eq. (1), on the other hand, suggests that the static resistance is the dominant component. The small component due to the mobile population will be useful in accounting for the stress-strain data, however, as we shall see.

The dynamics of the dislocation populations has been given consideration a number of times in the past. The model described here falls into the class of two-parameter models [7-9]; various one-parameter models, where no separation of the dislocations into mobile and static components is made, have also been proposed [10-12]. The basic premise is that under sufficient stress, mobile dislocations begin to move, which initiates strain and also the operation of multiplication sources. Some mobile dislocations tangle, however, adding to the static population. Additional changes may occur to the static population, such as recovery, but these operate over timescales beyond those of interest here. The

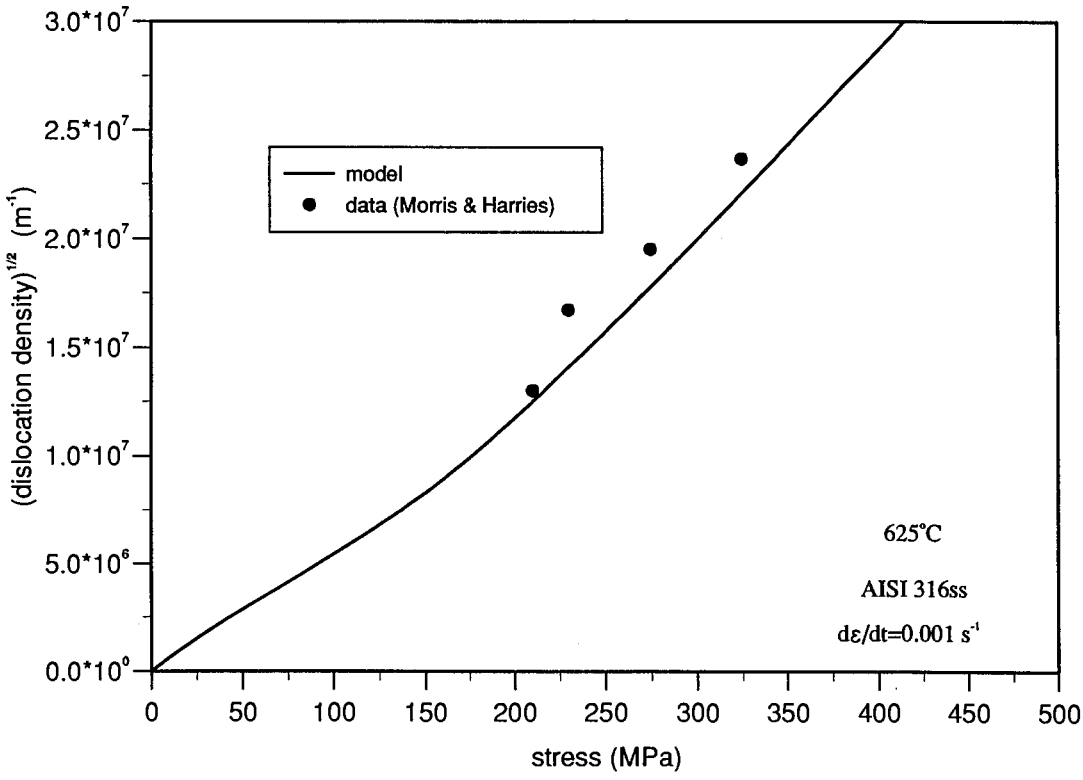

Figure 3. Dependence of dislocation density on applied stress during yield.

evolution equations are taken to be

$$\dot{\rho}_m = \mathcal{A}\dot{\epsilon} - \mathcal{B}\rho_m\dot{\epsilon} \quad , \tag{10}$$

$$\dot{\rho}_s = \mathcal{B}\rho_m\dot{\epsilon} \quad , \tag{11}$$

with $\mathcal{A}$ and $\mathcal{B}$ constants. In view of eq. (8), the terms on the right hand side of eq.(10) are, respectively, linear and quadratic in ρ_m. The equations are simple enough to allow analytic solution for a constant strain rate: the solutions are

$$\rho_m = \frac{\mathcal{A}}{\mathcal{B}}(1 - \exp -\mathcal{B}\epsilon) \quad , \tag{12}$$

and $\rho_s(\epsilon) = \rho_s(0) + \mathcal{A}\epsilon - \rho_m$. A boundary condition $\rho_m = 0$ when $\epsilon = 0$ has been used. These results can be compared directly with experimental data for AISI 316 steel [13] which exhibit a linear relationship between total dislocation density and yield strain, giving $\mathcal{A} = 4.5 \times 10^{15}$ m^{-2}. The same study yielded the dependence of the total dislocation density on stress during tensile deformation, shown in Figure 3. Using this data, it is possible to determine the other unknown parameters in eqs. (9) and (10). The resulting fit to the data is shown in Figure 3, and employs $\mathcal{B}$=120 and β_m=1: β_s is then determined by consistency with the fit given in eq. (1).

Using these parameters, it is possible to calculate the strain-hardening behaviour and to compare it with experiment. An example is shown in Figure 4 for a selected tensile test

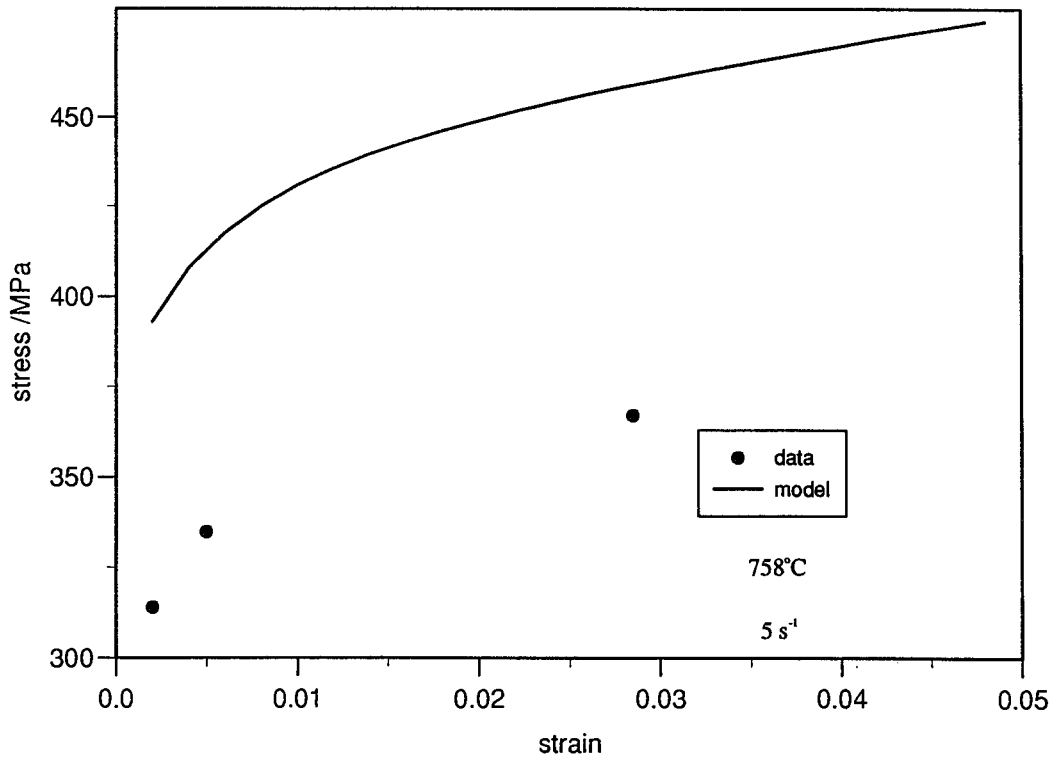

Figure 4. Stress-strain curve for irradiated AISI 316 steel: comparison between model predictions and data.

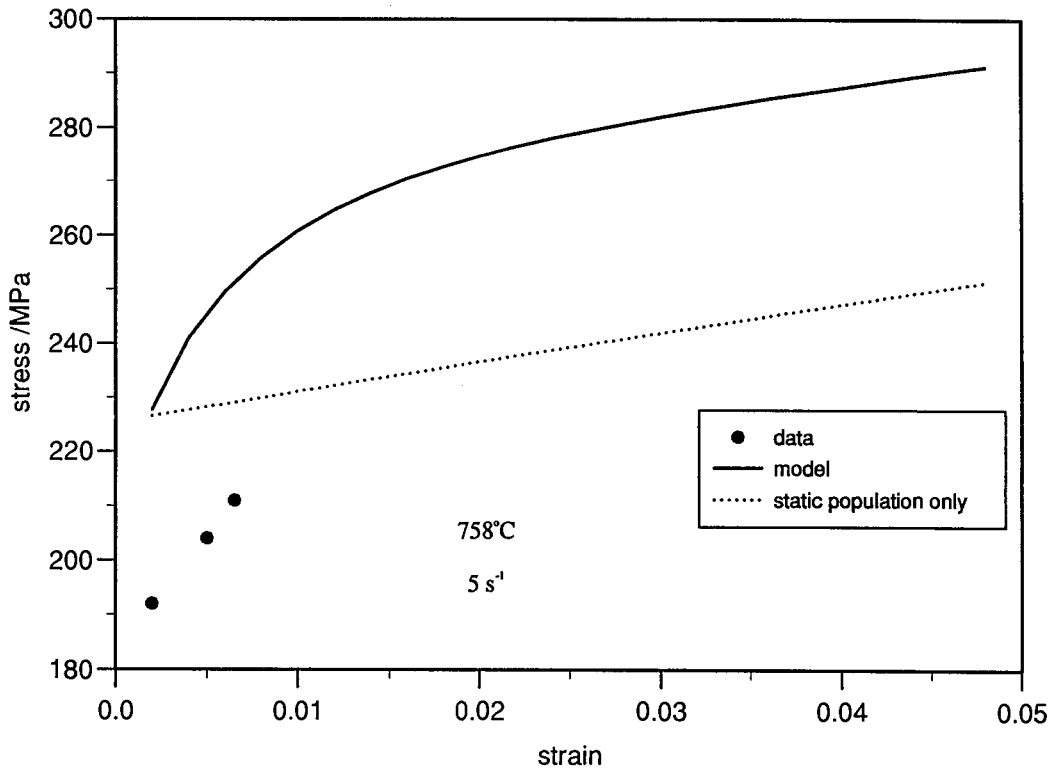

Figure 5. Stress-strain curve for test on irradiated AISI 316 steel: comparison between data and model with and without mobile dislocation component.

from the CABRI-1 programme. The material tested had been irradiated, which will have altered the yield stress to some extent, depending on the irradiation temperature. This is evident in the discrepancy between the experimental and predicted initial yield stresses. However, the model performs well in accounting for the initial steep rise in yield stress, which is due to the rapid initial increase in mobile dislocation density, before it saturates. A model without such a component would give rise to a much more shallow stress-strain curve at small strains. This is illustrated in Figure 5 which compares calculation with experiment for another test in the experimental programme. Although the curves typically under- or overpredict the yield stress by a small amount, which is evident in the linear fits in Figure 1, the strain-hardening behaviour is accounted for well.

4. CONCLUSIONS.

A previous model [2] of the evolution of the yield stress of fuel pin cladding materials has been extended, employing a better description of the physical processes responsible for the dependence on temperature, strain and strain rate. A simple model of dislocation mobilisation has been found sufficient to account for the main features of yield stress data for AISI 316 austenitic steel measured in tensile tests within the CABRI-1 programme [1]. The model involves two escape mechanisms which operate independently: the athermal bypassing of obstacles by the Orowan mechanism, and the thermally assisted penetration of the pinning points. The two mechanisms control yield at low and high temperature, respectively, and the different strain rate sensitivity of the yield stress in these two limits

emerges correctly. Tensile test data fit the expected theoretical form, using reasonable values of the various unknown physical quantities.

The strain-hardening behaviour of the material is accounted for using a simple two-population dislocation dynamics model. The dislocations are classed as either static or mobile. Each population makes characteristic contributions to the yield stress. When deformation is initiated, the mobile fraction increases from a low value, limited by a rate of immobilisation by tangling. The mobile population provides the strain whilst tangling increases the forces resisting further dislocation mobilisation, thus providing hardening. The resulting strain hardening agrees well with the observed stress-strain curves for the cladding. A treatment of a more extensive database of stress-strain curves is in preparation [3].

Extension of the model to allow for irradiation effects is straightforward. Radiation damage is considered to provide additional obstacles to dislocation motion [2] and a source term can be added to the evolution equation for the static dislocation population. The effects of recovery and recrystallisation can also be introduced within this population. Furthermore, the model offers the prospect of development into a unified model of material plasticity, taking into account both the creep and yield phenomena.

The model contains much that is physically realistic, but remains simple enough to pose no calculational problems. It can therefore be easily incorporated into complex fuel pin simulation codes, to describe the yield behaviour of fuel pin cladding in arbitrary deformation conditions.

ACKNOWLEDGEMENT.

This work was performed as part of the Fast Reactor Safety Programme of AEA Technology, funded by the U.K. Department of Trade and Industry.

REFERENCES.

1. M. Balourdet and R. Cauvin, "Transient mechanical properties of CABRI-1 cladding (CW 316)", Proc. BNES Conf. on Fast Reactor Core and Fuel Structural Behaviour, Inverness, 1990.

2. I.J. Ford, "Transgranular fracture of fast reactor irradiated stainless steel", *J. Nucl. Mat.* **182** (1991) 52.

3. I.J. Ford, "A dislocation model for plastic yield in austenitic stainless steels", in preparation.

4. U.F. Kocks, "A statistical theory of flow stress and work-hardening", *Phil. Mag.* **1966** 541.

5. A.J.E. Foreman and M.J. Makin, "Dislocation movement through random arrays of obstacles", *Phil. Mag.* **14** (1966) 911.

6. See, for instance, J.E. Dorn, "Low temperature dislocation mechanisms", in *Dislocation Dynamics*, (Eds. A.R. Rosenfield, G.T. Hahn, A.L. Bement, Jr., and R.I. Jaffee), McGraw-Hill, 1968.

7. G.B. Gibbs, "A general dislocation model for high temperature creep", *Phil. Mag.* **1966** 541.

8. G.M. Pharr and W.D. Nix, "Application of the methods of dislocation dynamics to describe plastic flow in both bcc and fcc metals", *Acta metall.* **27** (1979) 433.

9. Y. Estrin and L.P. Kubin, "Local strain hardening and nonuniformity of plastic deformation", *Acta metall.* **34** (1986) 2455.

10. Y. Estrin and H. Mecking, "A unified phenomenological description of work hardening and creep based on one-parameter models", *Acta metall.* **32** (1984) 57.

11. G. Gottstein and A.S. Argon, "Dislocation theory of steady state deformation and its approach in creep and dynamic tests", *Acta metall.* **35** (1987) 1261.

12. P.S. Follansbee and U.F. Kocks, "A constitutive description of the deformation of copper based on the use of the mechanical threshold stress as an internal state variable", *Acta metall.* **36** (1988) 81.

13. D.G. Morris and D.R. Harries, "Creep and creep rupture in a type 316 stainless steel at temperatures between 525°C and 900°C", Harwell report AERE-R 8811, June 1977.